

# Wireless Power Control Based on Large Language Models

Jiacheng Wang, *Graduate Student Member, IEEE*, Yucheng Sheng, *Graduate Student Member, IEEE*,  
Le Liang, *Member, IEEE*, Hao Ye, *Member, IEEE*, and Shi Jin, *Fellow, IEEE*

**Abstract**—This paper investigates the power control problem in wireless networks by repurposing pre-trained large language models (LLMs) as relational reasoning backbones. In hyper-connected interference environments, traditional optimization methods face high computational cost, while standard message passing neural networks suffer from aggregation bottlenecks that can obscure critical high-interference structures. In response, we propose PC-LLM, a physics-informed framework that augments a pre-trained Transformer with an interference-aware attention bias. The proposed bias tuning mechanism injects the physical channel gain matrix directly into the self-attention logits, enabling explicit fusion of wireless topology with pre-trained relational priors without retraining the backbone from scratch. Extensive experiments demonstrate that PC-LLM consistently outperforms both traditional optimization methods and state-of-the-art graph neural network baselines, while exhibiting exceptional zero-shot generalization to unseen environments. We further observe a structural-semantic decoupling phenomenon: Topology-relevant relational reasoning is concentrated in shallow layers, whereas deeper layers encode task-irrelevant semantic noise. Motivated by this finding, we develop a lightweight adaptation strategy that reduces model depth by 50%, significantly lowering inference cost while preserving state-of-the-art spectral efficiency.

**Index Terms**—Power control, interference management, large language model, fine-tuning.

## I. INTRODUCTION

The evolution toward sixth-generation (6G) wireless ecosystems envisions ubiquitous connectivity characterized by ultra-reliability and massive capacity. To support the heterogeneous spectrum of nodes—encompassing autonomous vehicles, industrial sensors, and extended reality (XR) hardware—ultra-dense network architectures have become indispensable. In particular, aggressive spatial reuse mechanisms, which allow multiple transceiver pairs to concurrently share the same frequency band, have emerged as a crucial strategy for maximizing spectral efficiency (SE) in such dense deployments. However, this inherent reliance on spatial reuse also creates severe interference coupling. The resultant hyper-connected environments are plagued by complex, mutual interference patterns that scale non-linearly with network density, making contention for limited spectral resources a major bottleneck.

Resource sharing requires judicious allocation for mitigating interference and optimizing resource utilization in ultra-dense

wireless networks. However, traditional resource allocation designs fall short in massive connectivity scenarios, where strictly coupled interference constraints pose a severe obstacle to deriving optimal solutions. In this context, mathematical optimization frameworks grounded in information theory and game theory have been extensively explored. Nevertheless, the objective of maximizing sum rates renders the power control problem non-convex and NP-hard. While classical iterative algorithms such as WMMSE [1] and FPLinQ [2, 3] can theoretically attain stationary points, they are plagued by prohibitive computational complexity and, more critically, numerical instability under stringent fairness constraints (e.g., harmonic utility). Consequently, reliance on such computationally intensive iterations becomes intractable for real-time applications as network density escalates.

As an effective tool to address problems of high dimensionality, deep learning (DL) has long been exploited for resource allocation design in wireless networks [4]. Architectures such as multi-layer perceptrons (MLPs) [5], convolutional neural networks (CNNs) [6], and deep reinforcement learning (DRL) frameworks [7] have been investigated to approximate optimization policies. More recently, graph neural networks (GNNs) have been further studied in [8–11] to exploit the permutation-equivariant property of wireless interference graphs. Similar system setups have been further considered in [12], where GNNs are utilized to enable efficient resource allocation. Despite these advances, many existing GNNs follow the message passing neural network (MPNN) paradigm with isotropic aggregation (e.g., sum or mean). In ultra-dense networks, where interference strengths can vary by several orders of magnitude, such aggregation creates a severe information bottleneck. By indiscriminately compressing diverse channel state information (CSI) from all user pairs into fixed-size node embeddings, MPNNs suffer from signal dilution, where critical strong interference patterns are numerically drowned out by the accumulation of weak interference [13]. This lossy compression imposes a performance ceiling, making it challenging for MPNN-based methods to consistently surpass traditional iterative benchmarks such as WMMSE [1].

In light of these limitations, the Transformer architecture [14] emerges as a compelling alternative to bypass the aggregation bottleneck. Through global self-attention, Transformers can directly model all-to-all interactions and capture complex relational dependencies without repeated and lossy local aggregation. Building upon this architectural advantage, large language models (LLMs) offer a further leap. Hav-

Jiacheng Wang, Yucheng Sheng, Le Liang and Shi Jin are with the School of Information Science and Engineering, Southeast University, Nanjing 210096, China (e-mail: wangjiacheng@seu.edu.cn; shengyucheng@seu.edu.cn; lliang@seu.edu.cn; jinshi@seu.edu.cn).

Hao Ye is with the Department of Electrical and Computer Engineering, University of California, Santa Cruz, CA 95064, USA (e-mail: yehao@ucsc.edu).

ing demonstrated unprecedented representational capabilities across language [15, 16] and vision [17] tasks, LLMs possess rich structural priors. We hypothesize that the relational structures learned during LLM pre-training can be repurposed for wireless interference modeling, since both language and wireless networks involve structured interactions among many entities, albeit in different modalities. Specifically, the ability of LLMs to capture complex, long-range contextual dependencies structurally mirrors the challenge of modeling non-local, mutual interference coupling. This perspective suggests that pre-trained LLMs may serve as general relational reasoning backbones for physical systems when appropriately adapted. Following this trend, recent studies in wireless communications have begun exploring LLM-based pipelines. The key obstacle, however, lies in the modality mismatch between continuous-valued wireless signals and the tokenized input interface of standard Transformer architectures. To mitigate this mismatch, several adaptation strategies have been proposed. For instance, a beam prediction framework has been proposed in [18], which adopts a hybrid input strategy to activate the model’s reasoning capabilities. Similar strategies have been further considered in [19], where learned CSI representations are embedded directly into the model to treat signal features as intrinsic inputs.

Despite these advancements, the potential of LLMs for medium access control (MAC) layer optimization remains largely unexplored. A key reason is that standard LLM architectures lack a native mechanism to effectively ingest interference topology. Unlike point-to-point physical-layer tasks, which primarily focus on signal reconstruction, MAC layer problems involve complex decision-making among interacting users, where the global interference topology is paramount. This creates a critical structural incompatibility: Standard Transformer attention is inherently feature-driven, relying on the dot-product similarity of latent embeddings. In wireless settings, however, the most important relationships are not necessarily between nodes with similar feature embeddings, but between nodes with strong physical interference coupling. Consequently, directly applying standard Transformer architectures to high-dimensional interference graphs can lead to severe information loss and sub-optimal resource orchestration.

To address this challenge and better harness the reasoning capabilities of LLMs for MAC layer optimization, we propose an interference-aware bias tuning mechanism that transforms a pre-trained LLM into a physics-informed graph Transformer. Drawing inspiration from AlphaFold2 [20], which successfully encoded 3D geometric constraints into attention mechanisms via pair biases, we adapt this paradigm to the wireless domain. Specifically, instead of relying solely on conventional feature embeddings, we inject the channel gain matrix directly into the self-attention module as an explicit physical bias term. This integration fundamentally reconfigures the attention landscape, compelling the model to prioritize nodes based on physical interference intensity rather than feature similarity. By selectively activating and fine-tuning the model’s shallow structural knowledge via low-rank adaptation (LoRA) [21], this approach efficiently strips away irrelevant semantic layers while retain-

ing the Transformer’s potent global reasoning capabilities. The main contributions of this paper are summarized as follows:

- We propose PC-LLM, a novel framework that repurposes pre-trained LLMs for MAC-layer power control. To overcome the topological blindness of standard Transformers, we design an interference-aware bias tuning mechanism that injects the channel gain matrix directly into the attention mechanism via a lightweight projector. This enables an efficient logit-level fusion of physical topology and pre-trained structural priors, bypassing the aggregation bottleneck of MPNNs.
- Extensive experiments demonstrate that PC-LLM consistently outperforms the optimal WMMSE benchmark and state-of-the-art GNN baselines across a wide range of network conditions. We further observe favorable scaling behavior regarding data heterogeneity, where learning from diverse scenarios improves generalization compared with models trained on a single distribution. Furthermore, PC-LLM possesses exceptional zero-shot robustness, maintaining high spectral efficiency even when extrapolated to unseen interference distributions without additional fine-tuning.
- We provide a pioneering analysis of the layer-wise modality alignment between LLMs and wireless physics. We uncover a critical structural-semantic decoupling: The relational reasoning required for interference management is concentrated in shallow layers, while deeper layers encode task-irrelevant linguistic semantics. This insight establishes a guideline for minimalist adaptation, allowing us to truncate the model significantly (e.g., by 50%) to reduce inference latency while preserving state-of-the-art performance.

The rest of the paper is organized as follows. In Section II, we provide a comprehensive review of the related literature regarding GNN-based resource management and the application of LLMs in wireless communications. Section III introduces the system model for wireless interference networks and formulates the power control optimization problem. Then, the proposed PC-LLM framework is presented in Section IV, where we detail the interference-aware bias tuning mechanism and the efficient training strategy. Simulation results are provided in Section V to validate the performance and generalization of our approach. Finally, the conclusion is drawn in Section VI.

## II. RELATED WORK

### A. GNN-based Resource Management

Owing to their inherent capability to capture topological structures and desirable scalability, GNNs have been extensively leveraged as the foundational architecture for next-generation network modeling. Theoretical frameworks have been established in [8], where resource management problems are formulated as graph optimization tasks underpinned by the universal permutation equivariance property. Building upon this theoretical basis, GNNs efficiently exploit spatial dependencies to facilitate scalable solutions. For combinatorial

problems such as link scheduling, graph embedding techniques have been investigated in [22] to maximize network throughput while significantly reducing the requisite training samples. More sophisticated architectures, such as GRLinQ [23] which integrates an MPNN with reinforcement learning, have demonstrated enhanced generalization capabilities and facilitated distributed execution. To bridge the gap between theoretical performance and practical deployment, recent efforts have focused on addressing signaling overhead and strict constraint satisfaction. To circumvent the dependency on full global CSI, a sparse graph isomorphism network is proposed in [24], utilizing an edge-sparsifying mechanism to report only critical CSI features. Simultaneously, to rigorously enforce constraints within learning-based frameworks, GNNs have been effectively integrated with primal-dual methods in [10, 11, 25]. Beyond static configurations, the adaptability of resource management policies to non-stationary environments has been improved through the fusion of meta-learning and GNNs [26]. Specifically, a modular meta-learning approach is explored in [27] to orchestrate power control in networks with arbitrarily time-varying topologies. For scenarios characterized by temporal shifts in CSI distribution, a meta-gating framework has been developed in [28], which dynamically weighs the importance of historical periods to ensure fast and continuous resource optimization.

Notwithstanding these strides, underlying standard MPNNs impose an inherent representational bottleneck, which often limits their ability to consistently surpass robust benchmarks like WMMSE [1] and FPLinQ [2]. We attribute this performance ceiling to the isotropic aggregation mechanism inherent in MPNNs. In fully connected interference graphs, this mechanism functions as a lossy compressor, forcing complex, high-entropy pairwise interactions into fixed-size node embeddings. This leads to a breakdown in injectivity [13], where distinct interference topologies become indistinguishable due to signal dilution. While the graph Transformer paradigm [29, 30]—exemplified by the success of AlphaFold2 [20] in biology—theoretically resolves these bottlenecks via global self-attention, training such high-capacity models from scratch entails prohibitive sample complexity. Furthermore, standard attention modules lack the native ability to encode continuous interference topology. These challenges motivate our pivot toward adapting pre-trained Transformer backbones, leveraging their established relational inductive bias to efficiently model the interference manifold without the cost of ground-up training.

## B. LLMs for Wireless Communication

Recent literature has extensively investigated alignment strategies for mapping wireless data into high-dimensional latent spaces compatible with pre-trained architectures [31]. Since standard LLMs operate on tokenized sequences, the dominant strategy involves projecting wireless features into embeddings that emulate discrete linguistic tokens. A representative framework is LLM4CP [19], which addresses channel prediction by normalizing and patching CSI sequences in the frequency-delay domain. These patches are subsequently

projected via a trainable neural network (NN) embedding layer into token vectors, allowing the LLM to process wireless data as pseudo-language sequences. In contrast, BP-LLM [18] introduces a dual-input paradigm: Natural language prompts are employed to trigger the model’s reasoning capability, while historical beam and angle-of-departure (AoD) sequences are converted into token-like embeddings via a trainable tokenizer. This mechanism effectively reformulates beam prediction as a next-token generation task. Recent literature has extensively investigated alignment strategies for mapping wireless data into high-dimensional latent spaces compatible with pre-trained architectures. Since standard LLMs operate on tokenized sequences, the dominant strategy involves projecting wireless features into embeddings that emulate discrete linguistic tokens. A representative framework is LLM4CP [19], which addresses channel prediction by normalizing and patching CSI sequences in the frequency-delay domain. These patches are subsequently projected via a trainable neural network (NN) embedding layer into token vectors, allowing the LLM to process wireless data as pseudo-language sequences. In contrast, BP-LLM [18] introduces a dual-input paradigm: Natural language prompts are employed to trigger the model’s reasoning capability, while historical beam and angle-of-departure (AoD) sequences are converted into token-like embeddings via a trainable tokenizer. This mechanism effectively reformulates beam prediction as a next-token generation task. Beyond single-task adaptations, recent works have explored multimodal and multi-task integration using similar tokenization principles. M2BeamLLM [32] proposes a unified encoding framework where heterogeneous data from sensors (e.g., LiDAR, GPS) and wireless links are fused and aligned into a single token sequence. Similarly, for multi-task physical-layer networks, [33] develops specialized LLM embedders that facilitate the simultaneous execution of precoding, signal detection, and channel prediction within a single pre-trained architecture.

Conversely, an alternative paradigm exploits the structural correlations between wireless channels and natural images to leverage pre-trained large vision models (LVMs). Unlike token-based methods that require learnable embedders, LVM4CSI [34] proposes a direct visualization strategy. By mapping numerical CSI matrices into RGB-compatible formats—either through colormaps or channel-wise mapping of real and imaginary parts—this approach enables the direct application of standard vision backbones (e.g., ConvNeXt) without extensive fine-tuning. Similarly, to address delay-Doppler estimation in mmWave systems, 2DLAM [35] employs a feature extraction module that converts delay-Doppler profiles into image-like embeddings compatible with ImageGPT. These visual alignment strategies effectively circumvent the need for complex tokenization, leveraging the inherent spatial pattern recognition capabilities of LVMs for wireless tasks.

Despite the extensive exploration of alignment strategies—ranging from token-based embeddings to visual transformations—these methodologies are predominantly tailored for signal-level physical-layer tasks. In contrast, MAC-layer optimization depends critically on interference topology, which is a relational structure more naturally captured by

graph-based models. How to effectively incorporate this non-Euclidean topology into the sequential reasoning pipeline of an LLM remains an open problem. In response, we propose logit-level modality alignment via an interference-aware bias tuning mechanism. This approach explicitly injects non-Euclidean topology into the LLM’s reasoning engine, imposing a physical structural bias upon the linguistic modality.

### III. SYSTEM MODEL AND PROBLEM FORMULATION

We consider the instantaneous power allocation problem in a single-hop wireless network comprising  $K$  single-antenna transceiver pairs that share a common frequency band. The network operates under a quasi-static block fading assumption, where the topology and channel gains remain invariant within a scheduling slot but vary independently across slots. Accordingly, this work focuses on snapshot-based resource optimization for given channel realizations.

Let  $h_{kj} \in \mathbb{C}$  denote the complex channel coefficient from transmitter  $j$  to receiver  $k$ . We distinguish between the direct link gain  $h_{kk}$  and the cross-link interference channel  $h_{kj}$  (for  $j \neq k$ ). The transmit power of the  $k$ -th transmitter is denoted by  $p_k$ , subject to a uniform maximum power budget  $P_{\max}$ . The global power allocation vector is defined as  $\mathbf{p} = [p_1, \dots, p_K]^T$ . Treating interference from concurrent transmissions as additive noise, the signal-to-interference-plus-noise ratio (SINR) at receiver  $k$  is given by

$$\text{SINR}_k(\mathbf{p}) = \frac{|h_{kk}|^2 p_k}{\sum_{j \neq k} |h_{kj}|^2 p_j + \sigma^2}, \quad (1)$$

where  $\sigma^2$  represents the noise power. The achievable SE for user  $k$  follows Shannon’s capacity formula, given by

$$R_k(\mathbf{p}) = \log_2(1 + \text{SINR}_k(\mathbf{p})). \quad (2)$$

The primary objective is to maximize a network-wide utility function subject to individual power constraints. Following the formulation in [36], the optimization problem is cast as

$$\begin{aligned} & \underset{\mathbf{p}}{\text{maximize}} && \sum_{k=1}^K \beta(R_k(\mathbf{p})) \\ & \text{subject to} && 0 \leq p_k \leq P_{\max}, \quad \forall k \in \{1, \dots, K\}, \end{aligned} \quad (3)$$

where  $\beta(\cdot)$  is a strictly increasing, concave utility function. Adopting specific forms of  $\beta(\cdot)$ , we target three distinct objectives:

- **Sum-Rate Maximization:** Setting  $\beta(z) = z$  maximizes the total network throughput. However, this objective inherently favors users with strong channel conditions, which frequently leads to the starvation of edge users.
- **Proportional Fairness:** Setting  $\beta(z) = \log(z)$  is equivalent to maximizing the geometric mean of user rates. This formulation facilitates a balanced trade-off between aggregate throughput and individual user fairness.
- **Harmonic Maximization:** Setting  $\beta(z) = -z^{-1}$  imposes severe penalties on low data rates. This metric enforces strict fairness and compels the system to prioritize the most disadvantaged links in the network.

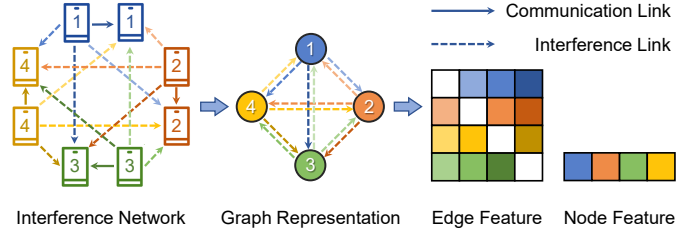


Fig. 1. Graph representation of the wireless interference network. Communication links within transceiver pairs are modeled as nodes, while the mutual interference between pairs is represented by directed edges, constituting a fully connected interference graph  $\mathcal{G}$ .

The optimization problem in (3) is non-convex and NP-hard due to the interference coupling in the SINR term. Classical approaches, most notably the WMMSE algorithm [1], address this challenge by iteratively optimizing a convex surrogate. While WMMSE is theoretically capable of accommodating any differentiable concave utility, its practical efficacy deteriorates significantly under strict fairness constraints. Specifically, the WMMSE update rules rely on auxiliary weights derived from the derivative of the utility function. For the harmonic utility  $\beta(z) = -z^{-1}$ , the derivative scales as  $z^{-2}$ . In high-interference regimes where the rates  $R_k$  of disadvantaged users can become very small, these weights exhibit hyperbolic growth. Such numerical hypersensitivity induces violent oscillations in the iterative updates, rendering the algorithm computationally intractable for real-time applications.

To circumvent these numerical pathologies, we propose a paradigm shift toward learning-based approaches that bypass iterative instability. Following the graph representation established in [8], we model the instantaneous interference topology as a fully-connected directed graph  $\mathcal{G} = (\mathcal{V}, \mathcal{E})$ , as illustrated in Fig. 1. Specifically, each node  $v_k \in \mathcal{V}$  represents the direct communication link within transceiver pair  $k$ , while each directed edge  $e_{kj} \in \mathcal{E}$  characterizes the interference link from transmitter  $j$  to receiver  $k$ . This graph-theoretic formulation explicitly captures the interference patterns that govern system utility, providing a structured topological foundation for the proposed PC-LLM framework.

### IV. PROPOSED PC-LLM FRAMEWORK

This section details the architecture of PC-LLM, a physics-informed framework tailored to repurpose pre-trained LLMs for wireless power control. As illustrated in Fig. 2, our approach diverges from the local filtering paradigm of standard MPNNs, adopting instead a global relational modeling strategy. While conventional MPNNs encounter severe capacity bottlenecks due to the indiscriminate compression of dense neighborhoods, our framework leverages the global self-attention mechanism to model complex all-to-all interference interactions. By maintaining a pairwise attention matrix, the model avoids the node-level aggregation bottleneck, allowing for selective processing of critical interference paths without lossy compression.

The framework is organized into a three-stage pipeline: 1) *Feature Construction*, which projects raw CSI into structured

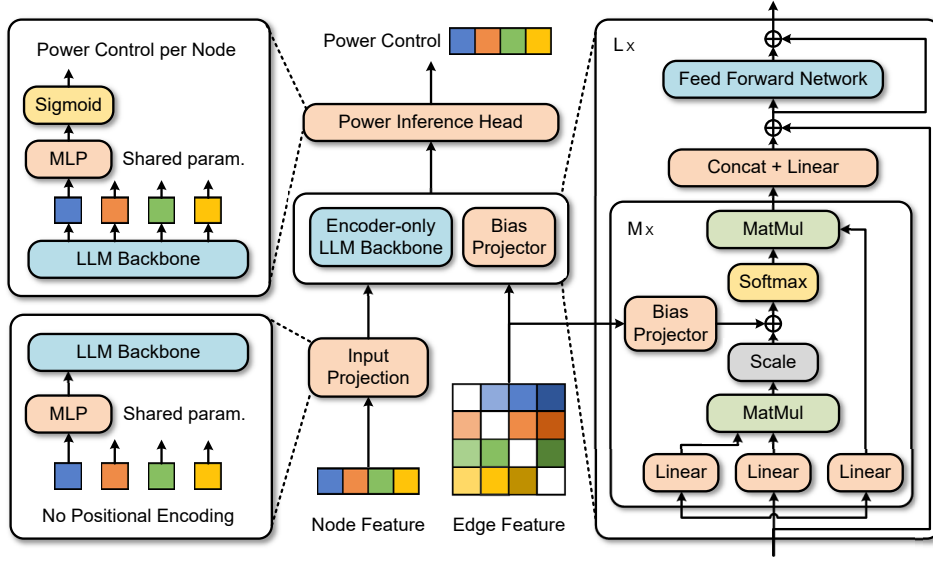


Fig. 2. Overall architecture of the proposed PC-LLM. The framework aligns physical channel features with the latent space of the model through an input projection layer, a bias-modulated Transformer backbone, and a power inference head. Red modules denote trainable components including task-specific layers initialized from scratch and pre-trained layers adapted via LoRA, while blue modules represent the frozen backbone.

graph attributes; 2) *Model Architecture*, comprising the embedding layers and the bias-modulated Transformer backbone; and 3) *Training Strategy*, which outlines the parameter-efficient adaptation process.

#### A. Feature Construction

To bridge the modality gap between high-dynamic-range wireless signals and the stable latent space of LLMs, we implement a unified preprocessing pipeline. Raw channel gains  $|h|^2$  are converted to the decibel (dB) scale and subsequently normalized to achieve zero mean and unit variance. We denote this element-wise transformation as  $\psi(|h|^2) = \text{norm}(10 \log_{10}(|h|^2))$ . Based on this protocol, we define the node and edge features for the interference graph  $\mathcal{G}$ .

**Node Feature.** Associated with each node  $v_k \in \mathcal{V}$ , the feature scalar  $s_k \in \mathbb{R}$  encodes the intrinsic physical state of transceiver pair  $k$ . It is defined as the normalized direct link strength  $s_k = \psi(|h_{kk}|^2)$ .

**Edge Feature.** Associated with each directed edge  $e_{kj} \in \mathcal{E}$ , the feature vector  $\mathbf{z}_{kj}$  characterizes the mutual interference coupling between transceiver pairs  $j$  and  $k$ . While the graph edge  $e_{kj}$  structurally denotes the unidirectional interference from transmitter  $j$  to receiver  $k$ , optimal power allocation necessitates an analysis of the bilateral interaction between the pair. Adopting the bidirectional modeling strategy from [9], we construct a composite feature that concatenates both the incoming interference strength and the reciprocal outgoing interference strength:

$$\mathbf{z}_{kj} = [\psi(|h_{kj}|^2), \psi(|h_{jk}|^2)]^\top \in \mathbb{R}^2. \quad (4)$$

In contrast to architectures that treat edges as independent tokens [29], this design maintains an input sequence length consistent with the node cardinality  $|\mathcal{V}| = K$ . These edge vectors  $\mathbf{z}_{kj}$  function as conditioning inputs for the bias projector,

explicitly modulating the attention weights between nodes  $v_k$  and  $v_j$  during the structural reasoning stage.

#### B. Model Architecture

The proposed architecture maps the constructed features to optimal power allocation decisions through a sequence of differentiable transformations.

**Input Projection.** Since the pre-trained Transformer backbone operates on high-dimensional tokens, the scalar node feature  $s_k$  requires projection. We employ a lightweight node encoder, implemented as a two-layer MLP, to map  $s_k$  into the hidden dimension  $d_{\text{model}}$ . Formally, the initial node embedding  $\mathbf{x}_k^{(0)} \in \mathbb{R}^{d_{\text{model}}}$  is computed as

$$\mathbf{x}_k^{(0)} = \mathbf{W}_2 \cdot \text{GELU}(\mathbf{W}_1 s_k + \mathbf{b}_1) + \mathbf{b}_2, \quad (5)$$

where  $\mathbf{W}_1 \in \mathbb{R}^{d_{\text{mid}} \times 1}$  and  $\mathbf{W}_2 \in \mathbb{R}^{d_{\text{model}} \times d_{\text{mid}}}$  are learnable weight matrices, while  $\mathbf{b}_1 \in \mathbb{R}^{d_{\text{mid}}}$  and  $\mathbf{b}_2 \in \mathbb{R}^{d_{\text{model}}}$  denote the corresponding bias vectors. These embeddings constitute the input matrix  $\mathbf{X}^{(0)} = [\mathbf{x}_1^{(0)}, \dots, \mathbf{x}_K^{(0)}]^\top \in \mathbb{R}^{K \times d_{\text{model}}}$ .

**LLM Backbone.** The sequence  $\mathbf{X}^{(0)}$  is fed into the pre-trained Transformer backbone. We specifically employ an encoder-only architecture utilizing bidirectional self-attention. This bidirectional context is essential for wireless networks, as the optimal strategy for any node is contingent upon the global interference state, rendering causal masking inappropriate. For the  $l$ -th layer, the input  $\mathbf{X}^{(l-1)}$  is projected into query, key, and value matrices for each attention head  $m$ , represented by

$$\begin{aligned} \mathbf{Q}^{(l,m)} &= \mathbf{X}^{(l-1)} \mathbf{W}_Q^{(l,m)}, \\ \mathbf{K}^{(l,m)} &= \mathbf{X}^{(l-1)} \mathbf{W}_K^{(l,m)}, \\ \mathbf{V}^{(l,m)} &= \mathbf{X}^{(l-1)} \mathbf{W}_V^{(l,m)}, \end{aligned} \quad (6)$$

where  $\mathbf{W}_{\{Q,K,V\}}^{(l,m)} \in \mathbb{R}^{d_{\text{model}} \times d_m}$  denote the projection matrices fine-tuned via LoRA,  $d_m = d_{\text{model}}/M$  represents the

dimension of each head, and  $M$  denotes the number of attention heads. To strictly enforce the permutation equivariance required for graph processing, we deliberately eliminate the positional encodings and the tokenizer from the standard LLM architecture. This modification ensures that the reasoning process is driven solely by the physical interference topology encoded in the biases.

**Interference-Aware Bias Injection.** Standard Transformers rely on content-based attention, where relationships are inferred primarily from node feature similarities. This mechanism suffers from topological blindness in wireless contexts, as interaction strength is governed by physical interference channels rather than latent feature dot-products. To address this limitation, we propose an interference-aware bias injection mechanism. Inspired by the pairwise-bias design in the Evoformer of AlphaFold2 [20], we explicitly map the interference topology into the self-attention calculation.

We introduce a learnable bias projector  $\phi^{(l)}(\cdot)$  for each layer, implemented as a separate MLP. It maps the edge feature  $\mathbf{z}_{kj} \in \mathbb{R}^2$  to a bias value  $B_{kj}^{(l,m)}$  for each head  $m$ . The projector is defined as

$$\begin{aligned} \phi^{(l)}(\mathbf{z}_{kj}) &= [B_{kj}^{(l,1)}, \dots, B_{kj}^{(l,M)}]^\top \\ &= \mathbf{W}_{\text{bias},2}^{(l)} \cdot \text{ReLU}(\mathbf{W}_{\text{bias},1}^{(l)} \mathbf{z}_{kj} + \mathbf{b}_{\text{bias},1}^{(l)}) + \mathbf{b}_{\text{bias},2}^{(l)}, \end{aligned} \quad (7)$$

where  $\mathbf{W}_{\text{bias},1}^{(l)} \in \mathbb{R}^{d_{\text{proj}} \times 2}$  and  $\mathbf{W}_{\text{bias},2}^{(l)} \in \mathbb{R}^{M \times d_{\text{proj}}}$  are learnable weight matrices, while  $\mathbf{b}_{\text{bias},1}^{(l)} \in \mathbb{R}^{d_{\text{proj}}}$  and  $\mathbf{b}_{\text{bias},2}^{(l)} \in \mathbb{R}^M$  denote the corresponding bias vectors. We initialize the output layer of the bias projector to zero so that all bias terms start from zero at the beginning of training. This allows the model to leverage the pre-trained attention distribution initially before gradually incorporating the physical interference constraints. The attention score between node  $k$  and node  $j$  at head  $m$  of layer  $l$  is modified as

$$A_{kj}^{(l,m)} = \frac{(\mathbf{q}_k^{(l,m)})^\top \mathbf{k}_j^{(l,m)}}{\sqrt{d_m}} + B_{kj}^{(l,m)}. \quad (8)$$

where  $\mathbf{q}_k^{(l,m)}$  and  $\mathbf{k}_j^{(l,m)}$  denote the query vector and the key vector for node  $k$  and node  $j$ , which correspond to the  $k$ -th and  $j$ -th row of matrices  $\mathbf{Q}^{(l,m)}$  and  $\mathbf{K}^{(l,m)}$ , respectively. The contextualized representation for layer  $l$  is subsequently computed by concatenating the outputs of  $M$  attention heads, followed by a linear projection, formulated as

$$\text{head}_m = \text{Softmax} \left( \mathbf{A}^{(l,m)} \right) \mathbf{V}^{(l,m)}, \quad (9)$$

$$\text{Attention}(\mathbf{X}^{(l-1)}) = \text{Concat}(\text{head}_1, \dots, \text{head}_M) \mathbf{W}_O^{(l)},$$

where  $\mathbf{W}_O^{(l)} \in \mathbb{R}^{d_{\text{model}} \times d_{\text{model}}}$  denotes the output projection matrix for layer  $l$ , which is also adapted via LoRA. By defining the bias as a function of physical channel gains, the model can prioritize interference-relevant interactions across layers while retaining the global relational reasoning capability of the pre-trained Transformer.

A critical advantage of this approach lies in its computational efficiency. While tokenizing  $K^2$  edges would result in an intractable  $\mathcal{O}(K^4)$  complexity, injecting topology directly into the attention logits preserves the  $\mathcal{O}(K^2)$  complexity

of standard self-attention. This ensures scalability to dense network environments typical of future wireless deployments.

**Power Inference Head.** Following propagation through  $L$  Transformer layers, the final latent representation  $\mathbf{x}_k^{(L)}$  encapsulates the local state of the node enriched by the global interference context. To map this high-dimensional vector to a feasible power level, we apply a power inference head followed by a Sigmoid activation  $\sigma(\cdot)$  scaled by the power budget, represented as

$$p_k = P_{\text{max}} \cdot \sigma \left( \mathbf{W}_{\text{out}}^\top \cdot \text{GELU}(\mathbf{W}_{\text{hid}} \mathbf{x}_k^{(L)} + \mathbf{b}_{\text{hid}}) \right), \quad (10)$$

where  $\mathbf{W}_{\text{hid}} \in \mathbb{R}^{d_{\text{hid}} \times d_{\text{model}}}$  and  $\mathbf{W}_{\text{out}} \in \mathbb{R}^{d_{\text{hid}} \times 1}$  constitute the learnable weights, with  $d_{\text{hid}}$  denoting the hidden dimension of the inference head.

### C. Training Strategy

The training process is designed to efficiently adapt the general-purpose Transformer backbone to the physical characteristics of wireless networks.

**Parameter-Efficient Fine-Tuning.** To mitigate the risk of overfitting and catastrophic forgetting while reducing memory overhead, we adopt LoRA [21] for parameter-efficient fine-tuning. Specifically, we freeze the entire pre-trained backbone and inject trainable low-rank decomposition matrices exclusively into the self-attention projection layers. For a specific pre-trained weight matrix  $\mathbf{W}_0 \in \mathbb{R}^{d_{\text{out}} \times d_{\text{in}}}$ , the update is formally expressed as

$$\mathbf{W} = \mathbf{W}_0 + \frac{\alpha}{r} \mathbf{W}_{\text{up}} \mathbf{W}_{\text{down}}, \quad (11)$$

where  $\mathbf{W}_{\text{down}} \in \mathbb{R}^{r \times d_{\text{in}}}$  and  $\mathbf{W}_{\text{up}} \in \mathbb{R}^{d_{\text{out}} \times r}$  denote the down-projection and up-projection matrices, respectively, with rank  $r \ll \min(d_{\text{in}}, d_{\text{out}})$ . The scaling factor  $\alpha$  is a constant hyperparameter balancing the pre-trained features and the task-specific adaptation. During training,  $\mathbf{W}_0$  remains fixed, and only the adapter matrices  $\{\mathbf{W}_{\text{down}}, \mathbf{W}_{\text{up}}\}$  are updated. This strategy allows PC-LLM to retain the robust feature extraction capabilities of the pre-trained model while learning task-specific patterns with minimal additional parameters.

**Discriminative Learning Rates.** We address the knowledge gap between the pre-trained backbone and the newly initialized components by applying discriminative learning rates [37]. Specifically, a higher learning rate is assigned to the node encoder, bias projector, and inference head to encourage rapid adaptation to physical features. Conversely, a lower learning rate is applied to the LoRA parameters to subtly refine the latent space of the backbone, ensuring that the pre-trained relational reasoning capabilities are not disrupted by high-variance gradients.

**Loss Function.** To enable the discovery of strategies that surpass suboptimal traditional algorithms, we adopt an unsupervised training objective. PC-LLM is trained to directly maximize the system utility defined in Section III. The loss function is defined as

$$\mathcal{L} = -\mathbb{E}_{\mathcal{G}} \left[ \sum_{k=1}^K \beta (R_k(\mathbf{p})) \right], \quad (12)$$

where  $\mathbf{p}$  is the power vector generated by the power inference head. Minimizing  $\mathcal{L}$  is therefore equivalent to maximizing the target utility (e.g., sum-rate, proportional fairness, or harmonic utility) in expectation over the training distribution.

## V. NUMERICAL RESULTS

### A. Experimental Details

1) *Simulation Settings*: To evaluate the robustness and generalization capabilities of the proposed framework under realistic deployment conditions, we employ the device-to-device (D2D) underlay network as a representative benchmarking scenario, generating a comprehensive dataset to simulate diverse interference topologies. The simulation environment covers a  $1000 \times 1000$  m<sup>2</sup> square region where  $K$  transmitter-receiver pairs are deployed.

**Topology Generation.** We employ a rigorous topology generation process to mirror practical network configurations. Transmitters are distributed according to a hard-core point process, which enforces a minimum separation distance of 30 m between nodes to prevent unrealistic physical overlap. Subsequently, a corresponding receiver is generated for each transmitter within a uniform ring area defined by the interval  $[d_{\min}, d_{\max}]$ . To ensure valid cell association, we enforce a strict nearest-neighbor policy where each receiver must be geographically closest to its serving transmitter. Receiver positions are regenerated if they violate this condition, thereby maintaining valid Voronoi tessellations and guaranteeing that every transmitter serves exactly one user. The channel model incorporates a dual-slope path loss component combined with log-normal shadowing (standard deviation  $\xi = 7$  dB) [11, 38], alongside Rayleigh fading to capture small-scale variations. The system operates over a bandwidth of  $W = 10$  MHz, with a maximum transmission power budget of  $P_{\max} = 10$  dBm and a noise power spectral density of  $-174$  dBm/Hz.

**Dataset Heterogeneity.** To foster robust generalization across diverse interference environments, we generate a heterogeneous dataset comprising 15 distinct scenarios. These scenarios are formed by the cross-combination of five user density levels  $K \in \{20, 35, 50, 65, 80\}$  and three transmitter-receiver distance ranges uniformly sampled from  $[d_{\min}, d_{\max}] \in \{[2, 65], [10, 50], [30, 70]\}$  m. This configuration creates a continuum of interference regimes, ranging from noise-limited sparse networks to interference-limited ultra-dense clusters. Each configuration comprises 70,000 network snapshots, partitioned into 50,000 for training, 10,000 for validation, and 10,000 for testing.

2) *Performance Metrics*: Consistent with the formulation in Section III, we evaluate the proposed framework using three distinct metrics. Although the training objective maximizes the aggregate network utility  $\sum \beta(R_k)$ , we report the corresponding mean user rates to provide physically interpretable insights normalized against the network size  $K$ :

- **Arithmetic Mean Rate**: Evaluates the sum-rate maximization task corresponding to  $\beta(z) = z$ .
- **Geometric Mean Rate**: Evaluates the proportional fairness task corresponding to  $\beta(z) = \log(z)$ .
- **Harmonic Mean Rate**: Evaluates the harmonic maximization task corresponding to  $\beta(z) = -z^{-1}$ .

3) *Network Hyperparameters and Training Details*: We employ BERT-Large [15] as the backbone for PC-LLM, comprising 24 Transformer layers with a hidden dimension of  $d_{\text{model}} = 1024$  and  $M = 16$  attention heads. To balance the performance and inference latency, we utilize the first 12 Transformer layers (the rationale for this depth selection is provided in Section V-D). We initialize the weights from the standard pre-trained BERT-Large checkpoint, and apply LoRA with a rank  $r = 16$  and a scaling factor  $\alpha = 32$  to the query, key, value, and output projection matrices.

**Optimization Configuration.** We adopt the discriminative learning rate strategy proposed in Section IV-C. The randomly initialized components (node encoder, bias projector, and inference head) are optimized with a learning rate of  $\eta_{\text{init}} = 1 \times 10^{-3}$  across all tasks. For the pre-trained backbone, the LoRA learning rate  $\eta_{\text{LoRA}}$  is tuned according to the optimization objective: We set  $\eta_{\text{LoRA}} = 1 \times 10^{-4}$  for the sum-rate maximization task, and  $\eta_{\text{LoRA}} = 3 \times 10^{-4}$  for the proportional fairness and harmonic maximization tasks. The model is trained using the Adam optimizer with a batch size of 512. We utilize an adaptive ReduceLRonPlateau scheduler that decays the learning rate by a factor of 0.5 upon validation stagnation (patience of 15 epochs), allowing the model to thoroughly exploit the optimization landscape.

**Numerical Stability.** Given the high dynamic range of interference power in ultra-dense networks, numerical stability is critical. We implement a two-tiered safeguard mechanism. First, for the proportional fairness and harmonic objectives, we enforce a lower bound on user rates,  $\bar{R}_k = \max(R_k, \epsilon)$  with  $\epsilon = 10^{-5}$ , to prevent infinite loss values during training. Second, we apply gradient clipping with a maximum norm of 1.0 during backpropagation. This constraint effectively counteracts the exploding gradient problem caused by the steep derivatives of the harmonic utility in low-rate regimes.

4) *Baselines*: To validate the efficacy of PC-LLM, we compare it against a spectrum of algorithms ranging from classical optimization methods to state-of-the-art learning-based approaches. To ensure a fair comparison regarding model capacity, we specifically introduce scaled-up versions of the deep learning baselines:

- **WMMSE [1]**: The classical WMMSE algorithm serves as the primary optimization benchmark, configured with a maximum of 100 iterations. Given the non-convex nature of the interference management problem, WMMSE is susceptible to initialization-dependent local optima. Therefore, we evaluate two variants: **WMMSE-Avg** reports the mean utility averaged over 100 independent random initializations, while **WMMSE-Best** selects the solution yielding the highest utility. Although computationally prohibitive for real-time applications, WMMSE-Best serves as an idealized performance upper bound for iterative optimization methods.
- **PCGNN [9]**: As a representative MPNN, we evaluate both the standard implementation and a scaled variant, denoted as **PCGNN-Large**. The latter expands the hidden dimensions of node and edge networks to 1024 (matching the embedding size of BERT-Large) and thereby increases the message dimension to 3072. This scaled variant is

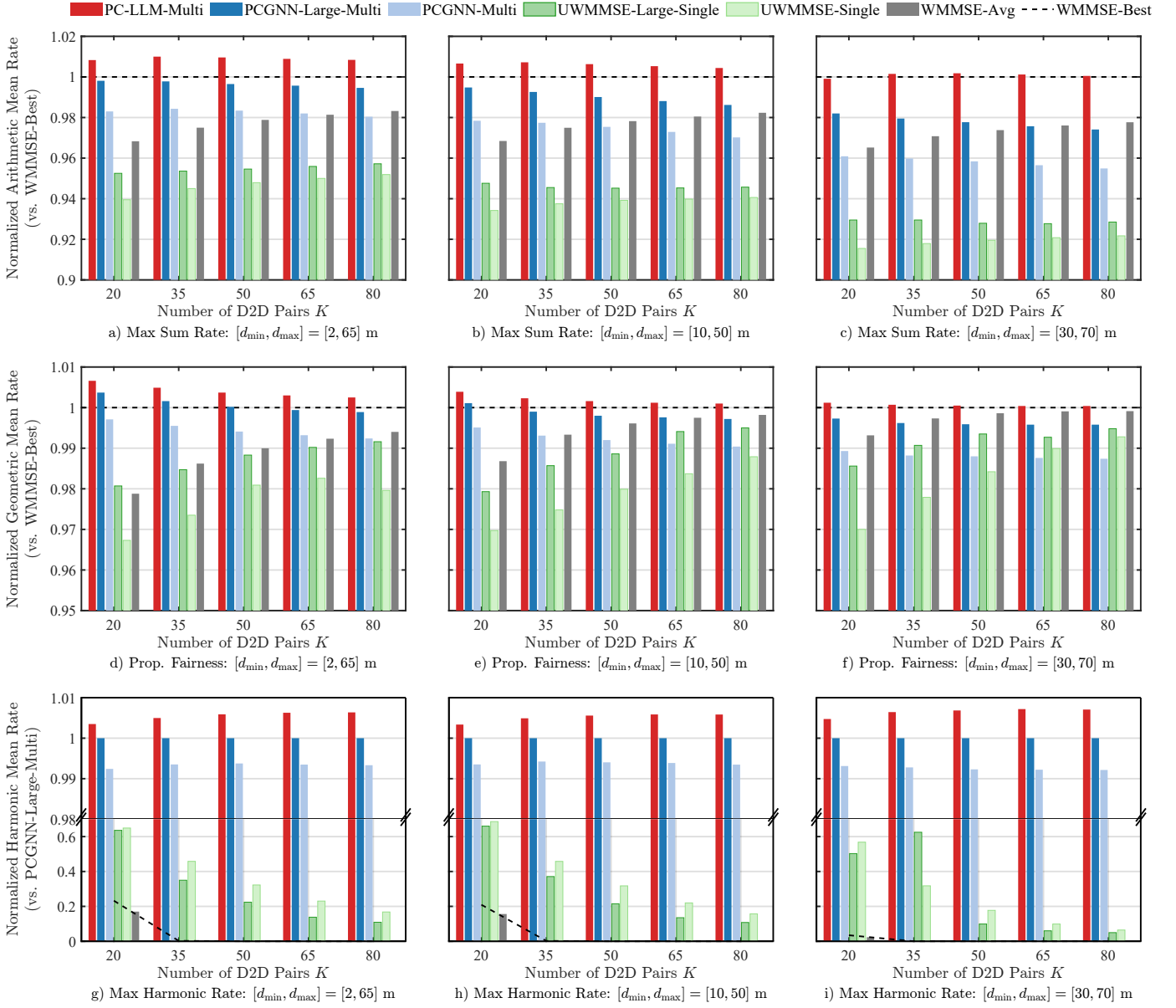


Fig. 3. Performance comparison of the proposed PC-LLM framework against baseline algorithms across varying network densities (number of D2D pairs  $K$ ) and interference environments (distance ranges  $[d_{\min}, d_{\max}]$ ). The results are organized by optimization objectives: (a)–(c) sum-rate maximization, (d)–(f) proportional fairness, and (g)–(i) harmonic maximization. The performance is normalized with respect to the WMMSE-Best algorithm for the max sum rate and proportional fairness tasks, whereas the harmonic mean rate is normalized relative to PCGNN-Large-Multi.

critical to decouple architectural benefits from parameter counts, verifying that the gains of PC-LLM stem from the proposed bias-tuning mechanism rather than mere model capacity.

- **UWMMSE [36]:** A deep unfolding framework that maps WMMSE iterations into a trainable MPNN architecture. We evaluate both the standard version and **UWMMSE-Large**, where the hidden dimensions of the internal graph convolutional modules are scaled to 1024 to align with the capacity of our proposed model.

Additionally, we include **Full Reuse** as a performance lower bound, where all transmitters operate at maximum power  $P_{\max}$ . This naive strategy is used primarily to quantify the severity of mutual interference and the potential gain offered

by power control schemes.

**Implementation Note:** WMMSE and UWMMSE are implemented using double-precision (`float64`) to mitigate numerical instability arising from their iterative updates. In contrast, end-to-end learning models (PC-LLM and PCGNN) demonstrate intrinsic stability and operate effectively with standard single-precision (`float32`).

## B. Performance Evaluation

Fig. 3 benchmarks the scalability of the proposed PC-LLM against baseline algorithms across varying network densities (number of D2D pairs  $K$ ) and interference environments (distance ranges  $[d_{\min}, d_{\max}]$ ). The evaluation is stratified by three distinct optimization objectives: sum-rate maximization in (a)–

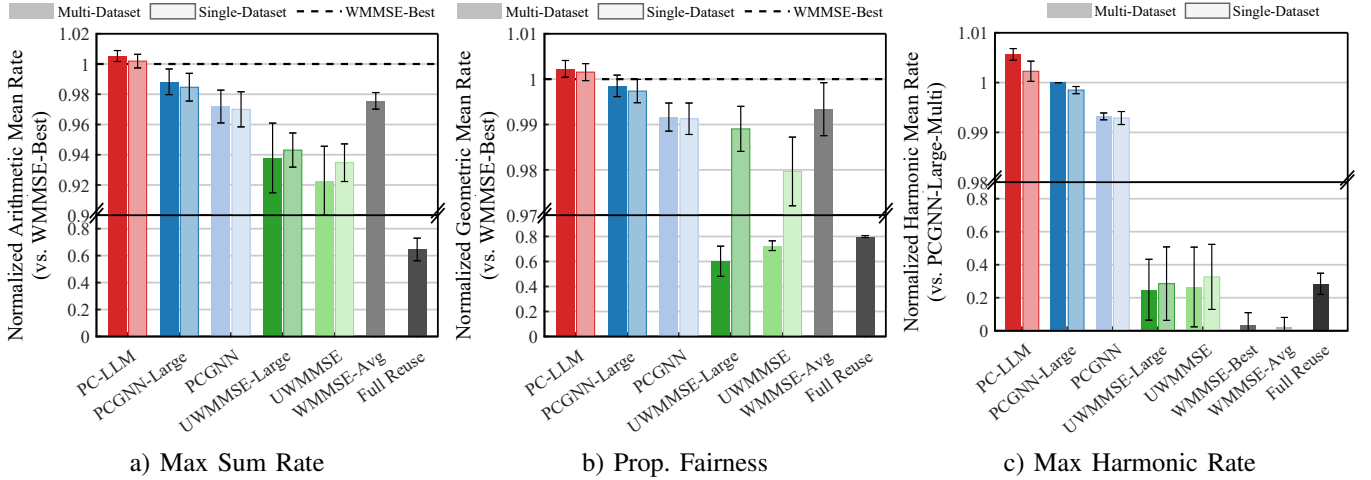


Fig. 4. Performance comparison of the proposed PC-LLM and baseline algorithms under multi-dataset and single-dataset training configurations. The performance is normalized with respect to the WMMSE-Best algorithm for the max sum rate and proportional fairness tasks, whereas the harmonic mean rate is normalized relative to PCGNN-Large-Multi. The bars represent the average performance across 15 distinct scenarios with varying user densities and channel distributions, while the error bars denote the standard deviation, indicating the robustness of each method.

(c), proportional fairness in (d)–(f), and harmonic maximization in (g)–(i). To ensure a rigorous comparison, performance metrics for the first two objectives are normalized with respect to the idealized WMMSE-Best algorithm. Conversely, for the harmonic maximization task, results are normalized relative to PCGNN-Large-Multi, an adjustment necessitated by the numerical instability of WMMSE in this regime. For clarity, each learning-based method in this figure reflects its optimal training configuration (either single- or multi-dataset), with the detailed impact of training data diversity explicitly decoupled and analyzed in Fig. 4.

Across the nine scenarios in Fig. 3, PC-LLM establishes a consistent dominance, stably surpassing the idealized WMMSE-Best benchmark across varying scales. As the network density increases, PC-LLM demonstrates superior robustness compared to baselines, which often suffer from performance degradation. Notably, the scaled-up baselines (PCGNN-Large and UWMMSE-Large) consistently outperform their standard counterparts, validating that increased model capacity contributes to performance gains. However, despite matching the parameter scale, PCGNN-Large still lags behind PC-LLM. This performance gap highlights that the superiority of PC-LLM stems not merely from model capacity, but fundamentally from the structural advantage of the proposed bias-tuned Transformer architecture over standard message-passing paradigms.

Specific to the sum-rate and proportional fairness tasks shown in Fig. 3(a)–3(f), most learning-based methods achieve competitive performance in sparse network configurations ( $K = 20$ ). However, as the network transitions into interference-limited regimes ( $K = 80$ ), the interference landscape becomes substantially more complex. In these high-density scenarios, MPNN-based baselines exhibit performance saturation. Resonating with our discussion in Section II-A, this limitation is attributed to the isotropic aggregation bottleneck inherent in MPNNs, forcing complex, high-entropy pairwise interference patterns into fixed-size node embeddings leads to signal dilution and a breakdown in injectivity. In contrast, PC-

LLM maintains a consistent lead. This indicates that the proposed interference-aware bias tuning mechanism effectively guides the Transformer to explicitly model critical interference paths within dense fully-connected graphs, avoiding the lossy compression observed in standard MPNNs.

The performance divergence is most pronounced in the harmonic maximization task shown in Fig. 3(g)–3(i), which imposes stringent fairness constraints. In this regime, we observe a sharp dichotomy between learning-based and optimization-based paradigms. While learning-based methods demonstrate inherent stability, with PC-LLM consistently outperforming the robust PCGNN-Large-Multi baseline, optimization-based approaches suffer drastic degradation. Corroborating our analysis in Section III, the collapse of WMMSE is attributed to numerical hypersensitivity: The derivative of the harmonic utility scales inversely with the square of the rate ( $z^{-2}$ ), causing auxiliary weights to exhibit hyperbolic growth when edge user rates approach zero. These violent oscillations render the iterative process unstable. Although UWMMSE employs a trainable unfolding network that partially mitigates this instability, it still fails to consistently surpass the naive full reuse baseline. In contrast, PC-LLM, as an end-to-end architecture, bypasses gradient-based auxiliary weight calculations, demonstrating exceptional numerical stability and effectively protecting disadvantaged users.

Finally, Fig. 4 investigates the impact of training data diversity by presenting the aggregate performance of PC-LLM and baselines under both single-dataset and multi-dataset training configurations. These results are averaged across 15 distinct interference scenarios, serving as a holistic benchmark for the scaling effects of different architectures. A distinct negative transfer phenomenon is observed for UWMMSE, where the multi-dataset model underperforms its single-dataset counterpart. This suggests that unfolding methods tend to overfit specific channel statistics and lack the flexibility to generalize across diverse environments. In contrast, PC-LLM demonstrates robust positive transfer, effectively leveraging heterogeneous data to refine its policy. It is imperative to

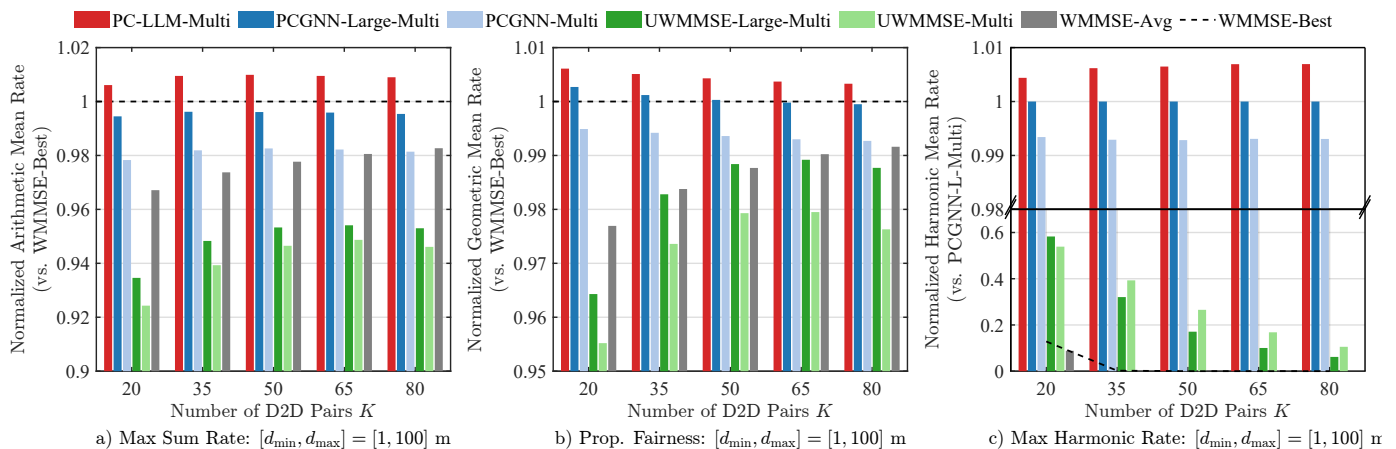


Fig. 5. Normalized generalization performance of multi-dataset trained models tested on the unseen wide-range scenario ( $[d_{\min}, d_{\max}] = [1, 100]$  m) with varying user densities  $K$ . The performance is normalized with respect to the WMMSE-Best algorithm for the max sum rate and proportional fairness tasks, whereas the harmonic mean rate is normalized relative to PCGNN-Large-Multi.

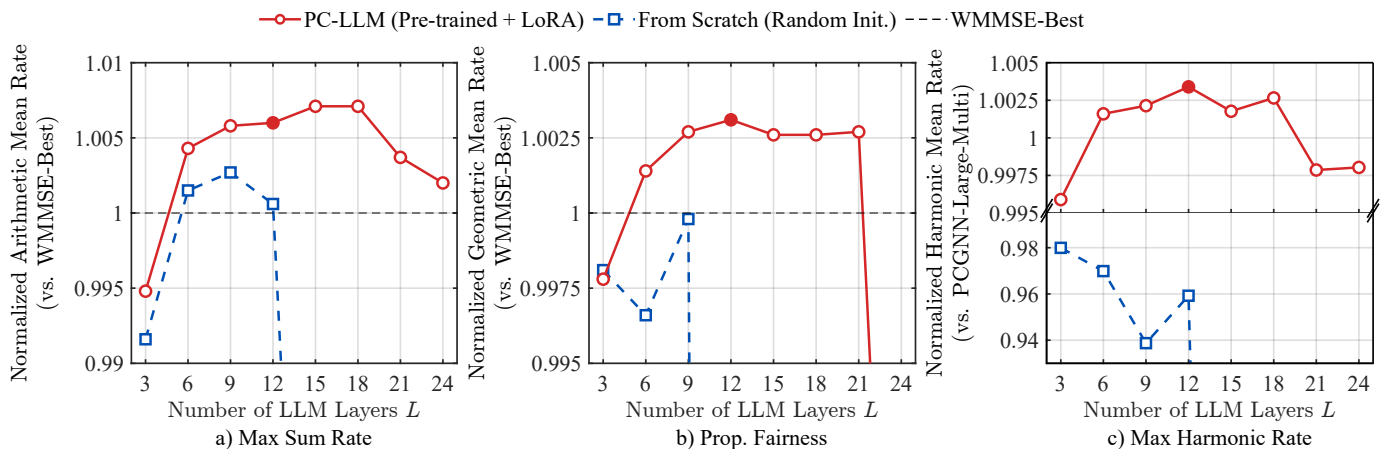


Fig. 6. Normalized performance comparison with varying number of LLM layers  $L$  under the setup of  $K = 50$  and  $[d_{\min}, d_{\max}] = [2, 65]$  m. The performance is normalized with respect to the WMMSE-Best algorithm for the max sum rate and proportional fairness tasks, whereas the harmonic mean rate is normalized relative to PCGNN-Large-Multi.

highlight the distinct nature of this gain: While PCGNN-Large improves upon a sub-optimal baseline, PC-LLM successfully demonstrates positive transfer even when its base performance is already near-optimal (i.e., outperforming WMMSE-Best). Securing further improvements in this high-performance saturation zone is significantly more challenging, validating that the Transformer backbone possesses a superior model capacity to push the performance boundary beyond strong specialized baselines. Furthermore, the error bars in Fig. 4(a) and 4(b) reveal a significant finding regarding stability. Despite the stochastic nature of channel realizations, PC-LLM exhibits remarkably narrow standard deviations, confirming that the model has learned a robust optimization policy that overcomes the initialization dependence typical of non-convex optimization algorithms.

### C. Generalization Analysis

Fig. 5 evaluates the zero-shot generalization capability of the proposed framework. The models trained on the standard heterogeneous dataset are deployed directly in an unseen scenario where the distance configuration parameters

$[d_{\min}, d_{\max}]$  are extended to  $[1, 100]$  m. This setting introduces a substantially broader dynamic range of interference power compared to the training phase. Despite this shift, PC-LLM demonstrates strong robustness and consistently outperforms the baselines across all tasks. Conversely, the UWMMSE baseline exhibits noticeable degradation, particularly in the harmonic maximization task. This performance divergence highlights the structural advantage of the proposed physics-informed graph Transformer. Global self-attention enables the model to capture all-to-all interactions directly, avoiding the information bottleneck inherent in standard MPNNs that compress diverse neighborhood information into fixed-size embeddings. Furthermore, interference-aware bias tuning explicitly integrates physical channel states into the attention calculation. By aligning attention scores with actual physical interference strength, the model learns a policy that is more closely grounded in wireless physics, rather than overfitting to the statistical artifacts of the training data. This ensures that the learned optimization strategy remains valid and efficient even when spatial configurations change significantly.

### D. Depth Analysis

Fig. 6 elucidates the impact of model depth  $L$  on optimization efficacy, evaluated under a representative dense interference environment characterized by  $K = 50$  pairs and a distance range of  $[2, 65]$  m. The results unveil a distinct inverted-U trend. Specifically, in the shallow regime ( $L = 3$  to 6), performance improves rapidly, indicating that a minimal reasoning depth is essential to capture the basic interference topology. This upward trend saturates around  $L = 12$ , forming a performance plateau where PC-LLM achieves state-of-the-art results across all objectives. However, as the depth extends further into the deeper regime ( $L > 18$ ), the performance trajectory reverses. A discernible degradation is observed as  $L$  approaches 24, particularly in the sum-rate and harmonic maximization tasks, where the normalized rates drop significantly below the peak levels. We attribute this subsequent saturation and degradation to a structural-semantic decoupling inherent in the hierarchy of LLMs. Early Transformer layers are known to emphasize general relational and dependency patterns, which are more transferable to wireless interference modeling. In our setting, these shallow layers appear to provide the most useful inductive bias for representing interaction topology among links. Conversely, deeper layers in pre-trained LLMs are increasingly specialized in abstract linguistic semantics, such as sentiment or complex reasoning. These semantic features constitute modal noise, creating a modality gap that interferes with the precise numerical regression required for wireless power control. Therefore, truncating the model at  $L = 12$  effectively filters out this noise while retaining the structural reasoning capabilities essential for topology management.

To isolate the contribution of pre-trained knowledge, we benchmark against a From Scratch baseline. In this configuration, the pre-trained weights are discarded in favor of random initialization, and the LoRA module is removed to permit full-parameter updates using a uniform learning rate  $\eta_{\text{init}}$ . As depicted in Fig. 6, a critical comparison reveals a profound performance gap: The randomly initialized counterpart not only converges to a substantially lower performance ceiling but also exhibits noticeable degradation as network depth increases. This empirical evidence confirms that the superior performance of PC-LLM stems not merely from the Transformer architecture itself but from the rich structural priors embedded in the pre-trained backbone. In the absence of these priors, the Transformer remains an architecture with a weak inductive bias that fails to spontaneously organize its attention mechanism for complex physical mappings when trained on limited wireless datasets. In contrast, the pre-trained structural priors provide a robust initialization that effectively guides the model through the highly non-convex optimization landscape of power control. Leveraging these established relational dependencies, PC-LLM successfully captures the underlying interference manifold, whereas the same task remains highly sample-inefficient and fails to reach competitive solutions when attempted from scratch.

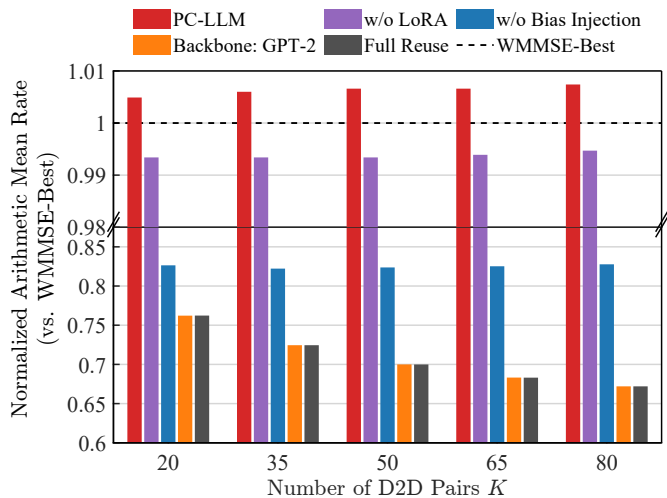


Fig. 7. Normalized ablation results of the proposed PC-LLM framework with varying number of D2D pairs  $K$  under the  $[d_{\min}, d_{\max}] = [2, 65]$  m scenario. The performance is normalized with respect to the WMMSE-Best algorithm.

### E. Ablation Studies

Fig. 7 presents an ablation study of the proposed framework to isolate the individual contributions of its core components: the backbone architecture, the interference-aware bias, and the LoRA fine-tuning strategy. The evaluation benchmarks the normalized performance across varying user densities  $K$  under the standard interference environment where transmitter-receiver distances are distributed within  $[2, 65]$  m.

First, we examine the structural foundation by replacing the bidirectional BERT-Large backbone with a unidirectional GPT-2-Medium (labeled “Backbone: GPT-2”). This substitution results in a catastrophic performance collapse, with rates degrading to the level of the naive full reuse baseline. This failure stems from a fundamental geometric mismatch between the model architecture and the physical problem. Wireless interference is inherently omni-directional and non-causal, forming a fully connected graph where every node interacts with every other node. In contrast, GPT-2 imposes a causal mask that enforces a strict left-to-right processing order, effectively severing the connectivity of the interference graph. Consequently, the bidirectional attention mechanism of BERT is proven to be not merely a capacity choice, but a structural necessity to preserve the mathematical isomorphism between the attention map and the physical interference topology.

Equally critical is the role of the proposed interference-aware bias. As observed in the “w/o Bias” configuration, removing this module causes the normalized rate to plummet precipitously, falling significantly below the WMMSE benchmark. This collapse confirms that standard self-attention is fundamentally topology-blind; without explicit positional or structural encoding, it treats the network as a permutation-invariant set rather than a spatial graph. The proposed bias is therefore decisive, as it injects the physical connectivity matrix directly into the attention mechanism. By modulating attention scores according to physical interference strength, it grounds the model’s reasoning in the real-world interference landscape, ensuring that the learned features distinguish dominant inter-

ferers from negligible noise.

Finally, we analyze the contribution of the training strategy by evaluating the “w/o LoRA” configuration, where the pre-trained backbone is frozen and only the bias module and projection heads are updated. Remarkably, the frozen model yields competitive performance hovering near the WMMSE-Best baseline, corroborating our earlier finding that pre-trained weights naturally possess robust structural reasoning capabilities. However, to consistently surpass the state-of-the-art, LoRA is essential for domain adaptation. It bridges the critical gap between the generic linguistic reasoning of the backbone and the specific numerical distributions of wireless channels. This adaptation transforms the model’s capability from qualitative structural analysis to the precise quantitative regression required for optimal power control.

## VI. CONCLUSION

In this paper, we have developed PC-LLM, a physics-informed framework that repurposes pre-trained LLMs as relational reasoning backbones for MAC-layer power control. To overcome the topological blindness of standard Transformers, an interference-aware bias tuning mechanism has been exploited to explicitly inject physical channel states into the attention module. We demonstrate that through this logit-level fusion of wireless topology and pre-trained structural priors, the proposed framework consistently outperforms optimal WMMSE and MPNN baselines with exceptional zero-shot robustness. Our analysis further reveals a critical structural-semantic decoupling, indicating that topology management relies primarily on shallow structural layers rather than deeper semantic ones. This work highlights the potential of wireless graph foundation models, envisioning a future paradigm where models are pre-trained directly on heterogeneous wireless graphs to encode universal physical laws for general-purpose wireless decision-making.

## REFERENCES

- [1] S. S. Christensen, R. Agarwal, E. de Carvalho, and J. M. Cioffi, “Weighted sum-rate maximization using weighted MMSE for MIMO-BC beamforming design,” *IEEE Trans. Wireless Commun.*, vol. 7, no. 12, pp. 4868–4877, Dec. 2008.
- [2] K. Shen and W. Yu, “Fractional programming for communication systems—Part I: Power control and beamforming,” *IEEE Trans. Signal Process.*, vol. 66, no. 10, pp. 2616–2630, May 2018.
- [3] —, “Fractional programming for communication systems—Part II: Uplink scheduling via matching,” *IEEE Trans. Signal Process.*, vol. 66, no. 10, pp. 2631–2644, May 2018.
- [4] Z. Qin, L. Liang, Z. Wang, S. Jin, X. Tao, W. Tong, and G. Y. Li, “AI empowered wireless communications: From bits to semantics,” *Proc. IEEE*, vol. 112, no. 7, pp. 621–652, Jul. 2024.
- [5] H. Sun, X. Chen, Q. Shi, M. Hong, X. Fu, and N. D. Sidiropoulos, “Learning to optimize: Training deep neural networks for interference management,” *IEEE Trans. Signal Process.*, vol. 66, no. 20, pp. 5438–5453, Oct. 2018.
- [6] W. Cui, K. Shen, and W. Yu, “Spatial deep learning for wireless scheduling,” *IEEE J. Sel. Areas Commun.*, vol. 37, no. 6, pp. 1248–1261, Jun. 2019.
- [7] L. Liang, H. Ye, and G. Y. Li, “Spectrum sharing in vehicular networks based on multi-agent reinforcement learning,” *IEEE J. Sel. Areas Commun.*, vol. 37, no. 10, pp. 2282–2292, Oct. 2019.
- [8] Y. Shen, Y. Shi, J. Zhang, and K. B. Letaief, “Graph neural networks for scalable radio resource management: Architecture design and theoretical analysis,” *IEEE J. Sel. Areas Commun.*, vol. 39, no. 1, pp. 101–115, Nov. 2020.
- [9] Y. Shen, J. Zhang, S. Song, and K. B. Letaief, “Graph neural networks for wireless communications: From theory to practice,” *IEEE Trans. Wireless Commun.*, vol. 22, no. 5, pp. 3554–3569, May 2023.
- [10] N. NaderiAlizadeh, M. Eisen, and A. Ribeiro, “State-augmented learnable algorithms for resource management in wireless networks,” *IEEE Trans. Signal Process.*, vol. 70, pp. 5898–5912, Dec. 2022.
- [11] —, “Learning resilient radio resource management policies with graph neural networks,” *IEEE Trans. Signal Process.*, vol. 71, pp. 995–1009, Mar. 2023.
- [12] Y. Dai, L. Lyu, N. Cheng, M. Sheng, J. Liu, X. Wang, S. Cui, L. Cai, and X. Shen, “A survey of graph-based resource management in wireless networks—Part II: Learning approaches,” *IEEE Trans. Cogn. Commun. Netw.*, vol. 11, no. 4, pp. 2101–2122, Aug. 2025.
- [13] K. Xu, W. Hu, J. Leskovec, and S. Jegelka, “How powerful are graph neural networks?” in *Proc. Int. Conf. Learn. Represent. (ICLR)*, May 2019.
- [14] A. Vaswani, N. Shazeer, N. Parmar, J. Uszkoreit, L. Jones, A. N. Gomez, Ł. Kaiser, and I. Polosukhin, “Attention is all you need,” in *Proc. Adv. Neural Inform. Process. Syst. (NeurIPS)*, Dec. 2017, pp. 5998–6008.
- [15] J. Devlin, M.-W. Chang, K. Lee, and K. Toutanova, “BERT: Pre-training of deep bidirectional Transformers for language understanding,” in *Proc. Annu. Meet. Assoc. Comput. Linguist. (NAACL)*, Jun. 2019, pp. 4171–4186.
- [16] T. B. Brown, B. Mann, N. Ryder, M. Subbiah, J. Kaplan, P. Dhariwal, A. Neelakantan *et al.*, “Language models are few-shot learners,” in *Proc. Adv. Neural Inform. Process. Syst. (NeurIPS)*, vol. 33, Dec. 2020, pp. 1877–1901.
- [17] A. Dosovitskiy, L. Beyer, A. Kolesnikov, D. Weissenborn, X. Zhai, T. Unterthiner, M. Dehghani *et al.*, “An image is worth 16x16 words: Transformers for image recognition at scale,” in *Proc. Int. Conf. Learn. Represent. (ICLR)*, May 2021.
- [18] Y. Sheng *et al.*, “Beam prediction based on large language models,” *IEEE Wirel. Commun. Lett.*, vol. 14, no. 5, pp. 1406–1410, May 2025.
- [19] B. Liu *et al.*, “LLM4CP: Adapting large language models for channel prediction,” *J. Commun. Inf. Netw.*, vol. 9, no. 2, pp. 113–125, Jun. 2024.
- [20] J. Jumper, R. Evans, A. Pritzel, T. Green, M. Figurnov, O. Ronneberger, K. Tunyasuvunakool, R. Bates, A. Žídek, A. Potapenko *et al.*, “Highly accurate protein structure prediction with AlphaFold,” *Nature*, vol. 596, no. 7873, pp. 583–589, Aug. 2021.
- [21] E. J. Hu, Y. Shen, P. Wallis, Z. Allen-Zhu, Y. Li, S. Wang, L. Wang, and W. Chen, “LoRA: Low-rank adaptation of large language models,” in *Proc. Int. Conf. Learn. Represent. (ICLR)*, Apr. 2022.
- [22] M. Lee, G. Yu, and G. Y. Li, “Graph embedding-based wireless link scheduling with few training samples,” *IEEE Trans. Wireless Commun.*, vol. 20, no. 4, pp. 2282–2294, Apr. 2021.
- [23] Z. Shan, X. Yi, L. Liang, C.-S. Liao, and S. Jin, “GR-LinQ: A hybrid model/data-driven spectrum sharing mechanism for device-to-device communications,” *IEEE Trans. Commun.*, vol. 73, no. 11, pp. 11 214–11 229, Nov. 2025.
- [24] K. Wang, H. Ye, L. Liang, and S. Jin, “Sparse graph neural networks for two-timescale wireless resource allocation,” in *Proc. IEEE Global Commun. Conf. Wkshps. (GLOBECOM Wkshps)*, Dec. 2023.
- [25] Y.-C. Liang, C.-S. Liao, and X. Yi, “A primal-dual algorithmic aspect of link scheduling in dynamic wireless networks,” in

- Proc. IEEE Int. Symp. Inf. Theory (ISIT)*, 2023.
- [26] B. Zhao, J. Wu, Y. Ma, and C. Yang, "Meta-learning for wireless communications: A survey and a comparison to GNNs," *IEEE Open J. Commun. Soc.*, vol. 5, pp. 1987–2015, Apr. 2024.
  - [27] I. Nikoloska and O. Simeone, "Modular meta-learning for power control via random edge graph neural networks," *IEEE Trans. Wireless Commun.*, vol. 22, no. 1, pp. 457–470, Jan. 2023.
  - [28] Q. Hou, M. Lee, G. Yu, and Y. Cai, "Meta-gating framework for fast and continuous resource optimization in dynamic wireless environments," *IEEE Trans. Commun.*, vol. 71, no. 9, pp. 5259–5273, Sep. 2023.
  - [29] V. P. Dwivedi and X. Bresson, "A generalization of Transformer networks to graphs," in *Proc. AAAI Workshop Deep Learn. Graphs: Methods Appl. (DLG-AAAI)*, Feb. 2021.
  - [30] C. Ying, T. Cai, S. Luo, S. Zheng, G. Ke, D. He, Y. Shen, and T.-Y. Liu, "Do Transformers really perform badly for graph representation?" *Proc. Adv. Neural Inform. Process. Syst. (NeurIPS)*, vol. 34, pp. 28 877–28 888, Dec. 2021.
  - [31] L. Liang, H. Ye, Y. Sheng, O. Wang, J. Wang, S. Jin, and G. Y. Li, "Large language models for wireless communications: From adaptation to autonomy," *arXiv preprint arXiv:2507.21524*, Jul. 2025.
  - [32] C. Zheng, J. He, C. G. Kang, G. Cai, Z. Yu, and M. Debbah, "M2BeamLLM: Multimodal sensing-empowered mmWave beam prediction with large language models," *arXiv preprint arXiv:2506.14532*, Jun. 2025.
  - [33] T. Zheng and L. Dai, "Large language model enabled multi-task physical layer network," *IEEE Trans. Commun.*, vol. 74, pp. 307–321, Oct. 2025.
  - [34] J. Guo, P. Jiang, C.-K. Wen, S. Jin, and J. Zhang, "LVM4CSI: Enabling direct application of pre-trained large vision models for wireless channel tasks," *arXiv preprint arXiv:2507.05121*, Jul. 2025.
  - [35] D. Xie, C. Liu, W. Wang, F. Guo, and X. Hu, "2DLAM: Joint delay-Doppler estimation in UAV mmWave system via large AI model," in *Proc. AAAI Wkshp. Artif. Intell. Wireless Commun. Netw. (AI4WCN)*, Mar. 2025.
  - [36] A. Chowdhury, G. Verma, C. Rao, A. Swami, and S. Segarra, "Unfolding WMMSE using graph neural networks for efficient power allocation," *IEEE Trans. Wireless Commun.*, vol. 20, no. 9, pp. 6004–6017, Apr. 2021.
  - [37] J. Howard and S. Ruder, "Universal language model fine-tuning for text classification," *arXiv preprint arXiv:1801.06146*, May 2018.
  - [38] X. Zhang and J. G. Andrews, "Downlink cellular network analysis with multi-slope path loss models," *IEEE Trans. Commun.*, vol. 63, no. 5, pp. 1881–1894, May 2015.